# *CHAPTER 3*

# Synthesis, Characterization and Antitumor Activity of Methotrexate-loaded Four-arm Star Poly(D,L-lactide)-*b*-Poly(*N*-vinylpyrrolidone) Amphiphilic Block Copolymer

## 3.1 Introduction

In recent years star-like polymers have attracted huge attention over simple linear polymers due to their unique solution and solid-state properties.[ Stenzel *et al*. (2001)] Star copolymers, compared to their linear analogs, contain central branching point with several polymeric arms which are interesting because they have impact on self-assembly of polymers, important to fabricate nano-structured materials.[Stenzel *et al*. (2001), Barner *et al*. (2003)] But micelles made of linear amphiphilic block copolymer may undergo dissociation in the blood stream on dilution and as a result unwanted early and rapid release of physically entrapped drug may occur. [Lawrence *et al*. (1995), Cao *et al*. (2011)] Sometimes drug-loaded such micelles have very large size which hindered their transport and biodistribution in tissues and organs. [Lawrence *et al*. (1995), Avgoustakis *et al*. (2004)] Moreover, such micelles have low drug loading capacity due to low hydrophobic interior space at their core part. [Wang *et al*. (2008), Zhou *et al*. (2015)] These drawbacks of such micelles can be overcome by developing an amphiphilic polymeric unimolecular micelle. Out of different approaches, [Wang *et a*l. (2005), Sheng *et al*. (2006), Prabaharan *et al*. (2009), Service *et al*. (1995), Liu *et al*. (1999), Kono *et al*. (1999), Bielinska *et al*. (2000), Rosen *et al*. (2009), Astruc *et al*. (2010)] use of multi-arm amphiphilic star block copolymer is one of the important approaches. Micelles of such multi-arm amphiphilic star block copolymers remains stable in selective media at relatively higher concentrations without association and at infinite dilution without dissociation. [Cao *et al*. (2011), Zhou *et al*. (2015)] Their size can be varied by changing the molecular weight of the star polymer core. [Cao *et al*. (2011), Zhou *et al*. (2015)] Their solubility in water can be varied by changing the ratio of the length of the hydrophobic core and the hydrophilic shell. [Cao *et al*. (2011),

Zhou *et al*. (2015)] Moreover, these micelles possess larger interior space to accommodate more drugs. [Cao *et al*. (2011), Ni *et al*. (2010)] Amphiphilic block copolymers containing both hydrophobic and hydrophilic segments have found many successful applications in the field of biomedical science owing to their tunable self-assembly property to generate nano-structured materials. The technique that is being widely used for the synthesis of well-defined amphiphilic block copolymers is controlled radical polymerization technique [Ouchi *et al*. (2009), Yamago *et al*. (2009)]. Such block copolymers self-assemble in water to form core/shell micellar nanoparticle (NP)s. The hydrophobic core is capable of carrying a variety of hydrophobic therapeutic agents and the hydrophilic coronas ensure biocompatibility of the NPs and water-solubility [Heise *et al*. (1999)]. Many applications like coating, colloid stabilization and drug delivery etc. were reported for such copolymers. [Kedar *et al*. (2010), Lee *et al*. (2006), Chen *et al*. (2009), Shin *et al*. (2009), Callewaert *et al*. (2005), Perelstein *et al*. (2010), Bulychev *et al*. (2004), Sakai *et al*. (2004)] In this regard, the reports of the synthesis of amphiphilic block copolymers containing a biocompatible hydrophilic poly(*N*-vinylpyrrolidone) (PNVP) segment and a biodegradable and biocompatible hydrophobic poly(D,L-lactide) (PDLLA) segment are very few in the literature. [Benahmed *et al.* (2001), Kang *et al*. (2004), Luo *et al*. (2004), Xiong *et al*. (2009)] and none involving controlled radical polymerization. In previous chapter we have reported for the first time, the synthesis of well-defined linear PDLLA-*b*-PNVP block copolymers through combination of ROP and well controlled xanthate mediated RAFT polymerization. To the best of our knowledge there is no report of star PDLLA-*b*-PNVP block copolymers so far. Here, I report for the first time the synthesis of well-defined four-arm star (PDLLA-*b*-PNVP)$_4$ block copolymers

[**Scheme 3.1)**] *via* combination of ROP and well controlled xanthate mediated RAFT polymerization. At first, a four-arm star PDLLA with –OH end-group [S-(PDLLA-OH)$_4$] was synthesized by ROP of DLLA using pentaerythritol as initiator. The –OH end-group was then converted to the corresponding –Br end group S-(PDLLA-Br)$_4$ through a reaction with 2-bromopropionyl bromide followed by the conversion of the –Br end-group to the corresponding *O*-ethyl xanthate end group S-(PDLLA-X)$_4$ through an ionic substitution reaction with potassium *O*-ethyl xanthate. Controlled/living radical polymerization of NVP was performed using the macro chain transfer agent S-(PDLLA-X)$_4$ and finally well-defined four-arm star amphiphilic Star-(PDLLA-*b*-PNVP)$_4$ block copolymers was synthesized. The polymers were characterized by $^1$H NMR and GPC studies. Self-assembly behavior of the resultant amphiphilic block copolymers was studied using $^1$H NMR, fluorescence spectroscopy, transmission electron microscopy (TEM), and dynamic light scattering (DLS) studies. MTX-loaded polymeric micelles of Star-(PDLLA$_{15}$-*b*-PNVP$_{10}$)$_4$ amphiphilic block copolymers were prepared and characterized by UV-Vis and TEM. MTX-loaded Star-(PDLLA$_{15}$-*b*-PNVP$_{10}$)$_4$ amphiphilic block copolymer micelles suppress lymphoma cells *in vitro* via apoptosis. Drug-loaded these micelles also suppress MTX resistant (MTX-R) lymphoma cells while free MTX remains ineffective. In addition, In addition, such drug-loaded micelles do not cause hemolysis compared to free MTX which is toxic for RBC.

## 3.2 Experimental Section

### 3.2.1 Materials

Pentaerythritol (Aldrich, St Louis, USA, 99%) are used as received. Other reagents are used as mentioned in the **2.2.1 section** of **Chapter 2**.

### 3.2.2 General methods

General methods are same as reported earlier in **Chapter 2**. The molecular weight of the PDLLA homopolymer from $^1$H NMR spectrum [$M_n$(NMR)] in DMSO-$d_6$ was determined by comparing the integrated peak intensity of aliphatic methylene protons of the backbone poly(D,L-lactide) chain at ~ 5.2 ppm (1H) to that of the methylene protons of the polymer chain-end at ~ 4.2 ppm (2H). The theoretical number-average molecular weight [$M_n$(theor)] of the resulted PDLLA-*b*-PNVP block polymer using S-(PDLLA-X)$_4$ xanthate macro chain-transfer agent was calculated using the following equation:

$$\overline{M}_n(\text{theor}) = \frac{[\text{NVP}]_o}{[\text{S-PDLLA-X}]_o} \cdot x_{\text{NVP}} \cdot M_{\text{NVP}} + M_{S\text{-PDLLA-X}}(\text{NMR})$$

where, $x_{NVP}$ is the fraction conversion of monomer, $M_{NVP}$ is the molecular weight of monomer, and $M_{S\text{-PDLLA-X}}$ (NMR) is molecular weight of the S-PDLLA-X xanthate macro chain-transfer agent determined from its $^1$H NMR.

### 3.2.3 Synthesis of Four-arm Star Poly(D, L-lactide)[S-(PDLLA$_{15}$-OH)$_4$] (run 1, Table 3.1)

Four-arm hydroxyl terminated star poly(D,L-lactide) [S-(PDLLA$_{15}$-OH)$_4$] was synthesized *via* the ROP of D,L-lactide using pentaerythritol as initiator and Sn(Oct)$_2$ as the catalyst. In a typical experiment, 6.0 g ($4.16\times10^{-2}$ mol) of D, L-lactide was placed

in a 100 mL Schlenk tube, and dried under vacuum at 80 ºC for 4 h. After cooling to RT, 0.24 g ($1.73\times10^{-3}$ mol) of pentaerythritol was added to the flask. Then, the reaction mixture was purged with nitrogen for 30 min. The Schelnk tube was then tightly closed, and heated to 150 ºC and 24 $\mu$L (0.5% of lactide, w/w) stannous octoate was injected into the reactor vessel and polymerization was continued at 150 ºC for 15 h. The polymerization was stopped by freezing the reaction mixture with liquid $N_2$. The crude product was dissolved in 10 mL THF and precipitated from 200 mL hexane. The precipitated polymer was collected by centrifugation. The separated polymer was purified by repeated dissolution in THF, precipitated from hexanes twice, and finally was dried under vacuum at RT for 24 h. Yield (gravimetric) = 5.34 g (89%), Conversion (%) (NMR) = 92%.

$^1$H NMR (300 MHz, DMSO-$d_6$) [**Figure 3.1(a)**]: $\delta$ (ppm) = 1.27 (d, $3H_e$), 1.44 (m, $3H_c$), 4.0-4.25 (m, $1H_d + 2H_a$), 5.1-5.2 (m, $1H_c$).

$M_n$(NMR) = 3,400 g mol$^{-1}$,$M_n$(GPC) = 7,000 g mol$^{-1}$, $M_w/M_n$= 1.24.

### 3.2.4 Synthesis of Four-arm Star [PDLLA-COCH(CH$_3$)Br]$_4$ [S-(PDLLA$_{15}$-Br)$_4$] (run 2, Table 3.1)

In a dried and nitrogen purged round-bottom flask, 4.5 g [$1.29 \times 10^{-3}$ mol, calculated on the basis of its $M_n$(NMR) = 3,400 g mol$^{-1}$] S-(PDLLA$_{15}$-OH)$_4$ were dissolved in 25 mL of dry THF with 2 mL ($1.29 \times 10^{-2}$ mol) triethylamine while stirring under nitrogen atmosphere. After that, 1.1 mL ($1.03 \times 10^{-2}$ mol) 2-bromopropionyl bromide was then added drop wise to the above-mentioned reaction mixture cooled in an ice bath. The reaction mixture was then stirred for 72 h at RT. The precipitated $Et_3N$.HBr salt was removed by filtration and filtrate was evaporated to dryness. The residue was dissolve in dichloromethane and washed thoroughly with 5% (w/v) aqueous sodium bicarbonate

solution (4 × 250 mL). The organic layer was further washed with water (4 × 300 mL), dried over anhydrous $Na_2SO_4$, and filtered. The filtrate was evaporated and died under vacuum at RT. The residue was re-dissolved in THF, precipitated with hexane, and dried under vacuum at RT for 24 h. Conversion (%) (NMR) = 100.

$^1$H NMR (300 MHz, DMSO-$d_6$): $\delta$ (ppm) = 1.46 (m, 3H$_c$), 1.74 (d, 3H$_g$), 4.76 (q, 1H$_f$), 5.1-5.2 (m, 2H$_b$), 4.16 (t, 2H$_a$)

$M_n$(NMR) = 4600 g mol$^{-1}$,$M_n$(GPC) = 5,200 g mol$^{-1}$, $M_w/M_n$ = 1.52

### 3.2.5 Synthesis of Four-arm Star [PDLLA-C(O)CH(CH$_3$)SC(S)OC$_2$H$_5$]$_4$ [S-(PDLLA$_{15}$-X)$_4$] (run 3, Table 3.1)

In a dried and nitrogen purged round-bottom flask, 4.0 g [7.66 × 10$^{-4}$ mol, calculated on the basis of its $M_n$(NMR) = 4,600g mol$^{-1}$] S-(PDLLA$_{15}$-Br)$_4$ and 0.5 g potassium *O*-ethyl xanthate (3.14 × 10$^{-3}$ mol) were degassed under nitrogen. In another dried and nitrogen purged round-bottom flask, 4.5 mL (5.5 × 10$^{-2}$ mol) pyridine was dissolved in 30 mL $CH_2Cl_2$ while stirring under nitrogen. This pyridine solution was added to the previous reaction mixture during stirring under nitrogen and stirring continued at RT for 36 h and finally diluted with 100 mL $CH_2Cl_2$. The solution was washed consecutively with saturated $NH_4Cl$ solution (4 × 50 mL), saturated $NaHCO_3$ solution (4 × 50 mL), and water (4 × 100 mL). The organic layer was dried over anhydrous $Na_2SO_4$, filtered and the filtrate was dried under vacuum at RT for 24 h. The residue was re-dissolved in THF, precipitated with hexane, and dried under vacuum at RT for 24 h. Conversion (%) (NMR) = 100.

$^1$H NMR (300 MHz, $CDCl_3$): $\delta$ (ppm) = 1.40-1.63 (m, 3H$_c$+3H$_g$+3H$_j$), 4.46 (q, 1H$_h$), 4.61-4.63 (q, 2H$_i$), 5.1-5.2 (m, 2H$_b$), 4.16 (t, 5H$_a$)

$M_n$(NMR) = 5,200 g mol$^{-1}$, $M_n$(GPC) = 8,500 g mol$^{-1}$, $M_w/M_n$ =1.55.

### 3.2.6 Typical Synthesis of Four-arm Star Block Copolymer Star-(PDLLA$_{15}$-b-PNVP$_{10}$)$_4$ (run 1, Table 3.2)

In a dried and nitrogen purged 30 mL Schlenk tube, 0.4 g [7.74× $10^{-5}$ mol, calculated on the basis of its $M_n$(NMR) = 5,200 g mol$^{-1}$] S-(PDLLA$_{15}$-X)$_4$ was dissolved in 4.0 mL THF. To it, 13.0 mg (7.74× $10^{-5}$ mol) AIBN and 0.83 mL (0.86 g, 7.74 × $10^{-3}$ mol) NVP were added. A homogeneous solution was obtained after stirring and it was degassed under nitrogen for 45 min. The Schlenk tube was then immersed in an oil bath preheated at 80$^o$C for 24 h. The reaction was stopped by freezing the reaction mixture with liquid nitrogen. A small portion of the polymerization mixture was used to determine the monomer conversion by $^1$H NMR. The remaining part of the polymerization mixture was dissolved in 10 mL THF, precipitated from 300 mL hexane, and dried under vacuum at RT for 24 h.

$^1$H NMR (300 MHz, $CDCl_3$): $\delta$ (ppm) = 1.2-1.9 (m, 12H$_c$+8H$_k$+12H$_g$ +12H$_j$), 1.9-2.0 (m, 8H$_q$), 2.2-2.4 (m, 8H$_r$), 3.0-3.5 (m, 8H$_p$), 3.6-3.9 (m, 4H$_l$), 4.2 (s, 8H$_a$), 5.2 (m, 8H$_b$).

$M_n$ (NMR) = 9,5300 g mol$^{-1}$, $M_n$(GPC) = 13,200 g mol$^{-1}$, $M_w/M_n$ = 1.32.

### 3.2.7 *In Vivo* Therapeutic Efficacy

AKR/J mice were maintained under pathogen-free condition of the central animal house facility of zoology department. Tumors (DL) in mice were maintained by transplanting fresh tumor cells in PBS (3×$10^4$ cells/mouse) intraperitoneally. All tumor measurements were made in a blinded fashion. Mice (n=12 /group) were transplanted with tumor, and after 96 h (Day 0) were administered intravenous with free MTX, MTX-loaded linear PDLLA$_{42}$-*b*-PNVP$_{63}$ or, star-(PDLLA$_{15}$-*b*-PNVP$_{10}$)$_4$ amphiphilic block copolymer micelles (3 mg kg$^{-1}$ body weight) or empty copolymers micelles in

PBS. Altogether 6 doses were given at an interval of 72 h. The formulations were prepared and validated so that 100 $\mu$l of PBS (vehicle) contain 3 mg $kg^{-1}$ body weight of MTX in MTX-loaded linear-PDLLA$_{42}$-*b*-PNVP$_{63}$ or, star-(PDLLA$_{15}$-*b*-PNVP$_{10}$)$_4$ micelles. The tumor volumes (abdominal circumference) and the body weights were monitored on a daily basis. The animals (n = 3) were sacrificed when the average abdominal circumference of the control (PBS only) exceeded 15.5 cm. Mice (n = 9/group) were under observation for 50 days when final data collection was made for Kaplan Mayer survival analysis and studying other immunological parameters.

### 3.2.8 Ethics statement

This study was performed in strict accordance with the recommendations for the care and use of laboratory animals of the National Regulatory Guidelines issued by the Committee for the Purpose of Supervision of Experiments on Animals (CPSEA), Ministry of Environment and Forest, Government of India. The protocol was approved by the Institutional Animal Ethics Committee, Banaras Hindu University. The animals were euthanized by cervical dislocation to reduce the sufferings as minimum as possible and was performed according to the AVMA Guidelines on Euthanasia (AVMA 2013).

## 3.3 Results and Discussion

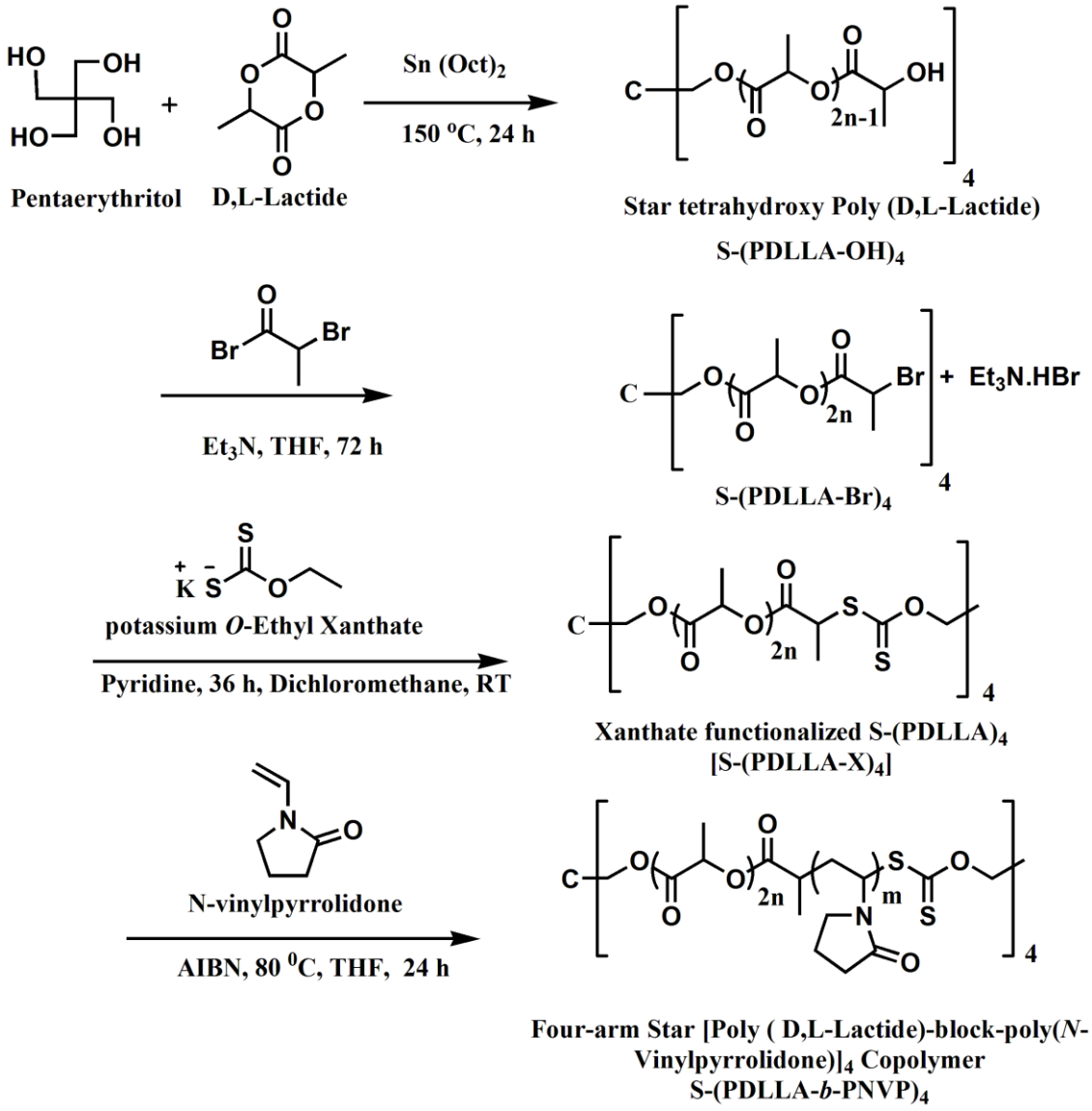


**Scheme 3.1** Synthesis of four-arm star block copolymer S-(PDLLA-*b*-PNVP)$_4$ by combined ROP and xanthate-mediated RAFT polymerization methods.

### 3.3.1 Synthesis of Four-arm Star Block Copolymers S-(PDLLA-*b*-PNVP)$_4$

The general synthetic procedure of four-arm star PDLLA-*b*-PNVP block copolymer is described in **Scheme 3.1**. It was synthesized *via* the combination of ROP and xanthate-mediated RAFT polymerization. In the first step, well-defined four-armed S-(PDLLA-

$OH)_4$ was successfully synthesized by ROP in bulk at 150 $^oC$ in the presence of $Sn(Oct)_4$ catalyst using the feed ratio of DLLA monomer and pentaerythritol initiator at 24 (**run 1**, **Table 3.1**). $^1H$ NMR [**Figure 3.1(A)**] confirms clearly its formation. Unimodal GPC chromatogram with $M_n$(GPC) = 7,000 g $mol^{-1}$ and $M_w/ M_n$= 1.24 is observed for the resultant star polymer [**Figure 3.2(a)**]. The corresponding molecular weight calculated from its $^1H$ NMR [$M_n$(NMR)] [**Figure 3.1(A)**] is 3,400 g $mol^{-1}$. The observed higher molecular weight in GPC measurement may be due to the star shape of the polymer and the use of the PMMA standards for calibration.

The –OH end groups in S-(PDLLA-$OH)_4$ were then converted into the corresponding bromides [S-(PDLLA-$Br)_4$] on reaction with 2-bromopropionyl bromide in the presence of triethyl amine (**run 2**, **Table 3.1**). The incorporation of the 2-bromopropionyl group is evidenced from the appearance of methine '*f*' and methyl '*g*' protons of 2-bromopropionyl end-group of the PDLLA-Br at around 4.72 and 1.72 ppm, respectively [**Figure 3.1(B)**]. The calculated conversion (%) of –OH end-group into its corresponding 2-bromopropionyl end-group obtained by comparing the peak area of methyl '*g*' protons of 2-bromopropionyl end-group with that of the methylene proton '*a*' of the polymer chain-end at ~ 4.2 ppm is ~ 100%.

**Table 3.1 Synthesis of Four-arm Star-(PDLLA-$X)_4$ Macro-chain Transfer Agent.**

| Run | Sample | Conv(%)[d] (nmr.) | $M_n$[d](NMR) g $mol^{-1}$ | $M_n$[e](GPC) g $mol^{-1}$ | PDI [e] (GPC) | Coments |
|---|---|---|---|---|---|---|
| 1 | S-(PDLLA-$OH)_4$ [a] | 92 | 3,400 | 7,000 | 1.24 | Unimodal |
| 2 | S-(PDLLA-$Br)_4$ [b] | 100 | 4,600 | 5,200 | 1.52 | Unimodal |
| 3 | S-(PDLLA-$X)_4$ [c] | 100 | 5,200 | 8,500 | 1.55 | Unimodal |

[a] Bulk polymerization using 6.0 g (41.6 m mol) LA, 30 mg ($7.4x10^{-5}$ mol) $Sn(oct)_2$) in the presence of pentaerythritol at 150 $^oC$ for 16 h;

[b] Using S-(PDLLA-$OH)_4$ : triethylamine : 2-bromopropionylbromide : 1: 2.5 : 2 in THF at RT for 72 h;

[c] Using S-(PDLLA-$Br)_4$ : potassium *O*-ethyl xanthate : pyridine :: 1 : 3 : 53 in dichloromethane (DCM) at room temperature for 36 h

[d] Determined by $^1H$ NMR.

[e] Determined by GPC (DMF, 0.5 mL/min, 40 $^oC$) calibrated against PMMA standards.

The $M_n$(NMR) of this polymer calculated by dividing average peak area of methylene protons '*b*' of the PDLLA backbone chain by the peak area of '*a*' is 4,600g mol$^{-1}$.

The corresponding observed unimodal GPC chromatogram has $M_n$(GPC) and PDI values of 5,200 g mol$^{-1}$ and 1.52, respectively [**Figure 3.2(a)**]. It is to be noted here that similar observed lower $M_n$(GPC) for 2-bromopropionyl end-functionalized PDDLA and PCL polymers was also observed by us earlier [Mishra *et al.* (2011), Mishra *et al*. (2013)].

S-(PDLLA$_{15}$-Br)$_4$ polymer was further reacted with potassium-*O*-ethyl xanthate to convert the bromo end-group into their corresponding xanthate [S-(PDLLA$_{15}$-X)$_4$] by ionic substitution reaction (**run 3**, **Table 3.1**). The conversion of bromo end-group into the corresponding xanthate end-group is confirmed by the appearance of the new characteristic peak attributed to the methylene proton '*f*' of the xanthate end group at 4.6 ppm [**Figure 3.1(C)**]. The corresponding peaks of the methyl protons '*h*' of the xanthate end-group and '*g*' of the propionyl group are overlapped within the peak of the methyl protons '*c*' of the PDLLA backbone chain. The calculated conversion (%) (from its $^1$H NMR) of –Br end-group into its corresponding xanthate end-group obtained by comparing peak area of methine protons '*g*' of the propionyl group with that of the methylene protons '*f*' of the xanthate end-group is ~ 100%. In addition, the characteristic UV absorption peak of the -S-(C=S)- functional group of the xanthate chain end-group of the resulted star polymer S-(PDLLA$_{15}$-X)$_4$ was observed in its THF solution at $\lambda$ ~ 280 nm. The observed $M_n$ (NMR) of this polymer calculated from its $^1$H NMR [**Figure 3.1(C)**] by dividing the peak area of '*b*' by the peak area of '*h*' is 5,200 g mol$^{-1}$. The corresponding observed unimodal GPC chromatogram has $M_n$ (GPC) and PDI values of 8,500 g mol$^{-1}$ and 1.55, respectively [**Figure 3.2(a)**].

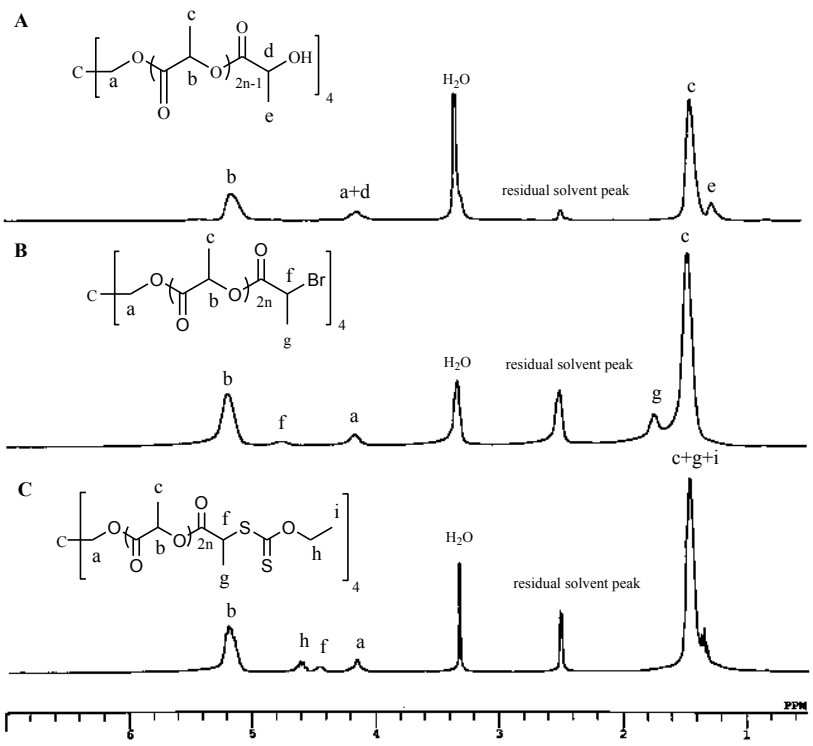


**Figure 3.1**. $^{1}$H NMR spectra of (**A**) S-(PDLLA$_{15}$-OH)$_4$, (**B**) S-(PDLLA$_{15}$-Br)$_4$ and (**C**) S-(PDLLA$_{15}$-X)$_4$ in DMSO-$d_6$ at room temperature.

The xanthate mediated RAFT polymerization of NVP was then performed using S-(PDLLA-X)$_4$ macro-chain transfer agent and AIBN initiator at 1: 1 molar ratio in THF at 80 $^{o}$C for 24 h. The results of the synthesis and characterization of S-(PDLLA-*b*-PNVP)$_4$ block copolymers from the corresponding S-(PDLLA-X)$_4$ macro-chain transfer agent are shown in **Table 3.2**. **Runs 1**, **2** and **3** correspond to 100, 200, and 300 equivalents of NVP monomer loading with respect to S-(PDLLA$_{42}$-X)$_4$ macro-chain transfer agent, respectively. Unimodal GPC chromatograms are obtained. Molecular weights of the resulted block copolymers are increased with the increase in the monomer loading as expected [**Figure 3.2(b)**].

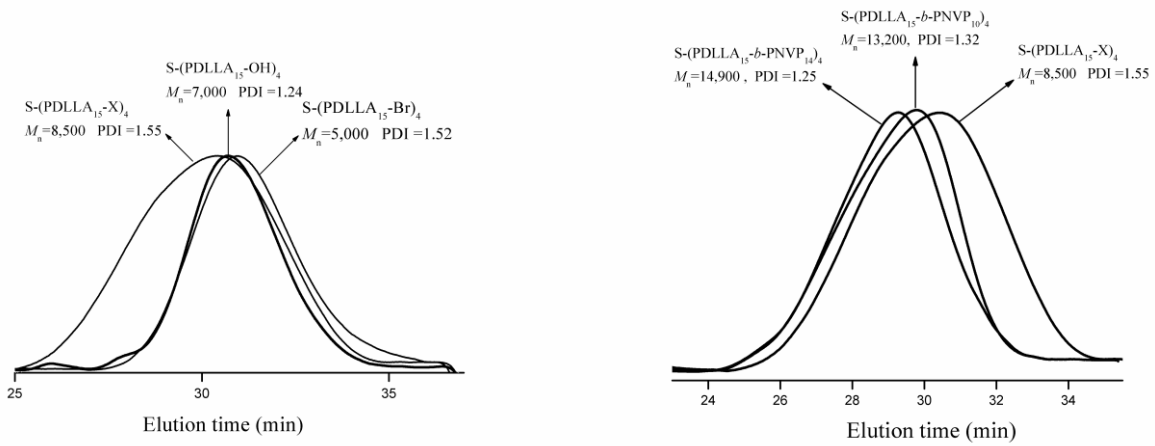


**(a)** **(b)**

**Figure 3.2 (a)** Gel Permeation Chromatograms of S-(PDLLA$_{15}$-OH)$_4$, S-(PDLLA$_{15}$-Br)$_4$ and S-(PDLLA$_{15}$-X). **(b)** Gel Permeation Chromatograms of S-(PDLLA$_{15}$-X) macro-chain transfer agent and resulted star block copolymers of S-(PDLLA-*b*-PNVP)$_4$ (**Table 3.2**)

**Table 3.2 Synthesis and Characterization Data of S-(PDLLA-*b*-PNVP)$_4$ Block Copolymers[a]**

| Run | Block copolymer | NVP[b] (equi.) | Convn.[c] (NMR) | $M_n$[d] (theor.) | $M_n$[e] (NMR) | $M_n$/PDI[f] (GPC) | $X_{NVP}$[g] (GPC) | $X_{NVP}$[g] (NMR) | CMC[h] (mg/L ) |
|---|---|---|---|---|---|---|---|---|---|
| 1 | S-(PDLLA$_{15}$-*b*-PNVP$_{10}$)$_4$ | 100 | 18.4 | 7,200 | 9,500 | 13,200/1.32 | 0.35 | 0.46 | 3.64 |
| 2 | S-(PDLLA$_{15}$-*b*-PNVP$_{14}$)$_4$ | 200 | 21.3 | 9,900 | 12,100 | 14,900/1.25 | 0.43 | 0.57 | 5.14 |
| 3 | S-(PDLLA$_{15}$-*b*-PNVP$_{15}$)$_4$ | 300 | 13.4 | 9,630 | 13,500 | 15,400/1.24 | 0.44 | 0.62 | 5.81 |

[a] Using 1 equivalent AIBN with respect to S-(PDLLA$_{15}$-X)$_4$ macroinitiator in THF at 80 $^o$C for 24 h;
[b] With respect to S-(PDLLA$_{15}$-X)$_4$ macro-chain transfer agent;
[c] Conversion was determined by using $^1$H NMR comparing the peak area of the residual vinylic sigments of the NVP monomer at ~ 4.3 - 4.4 ppm (2H) and ~7.0 - 7.1ppm (1H) with that of the methylene proton of the PNVP block of the polymer ;
[d] $M_n$(theor) = $^1$H NMR mol. wt. of S(PDLLA$_{15}$-X)$_4$ + ([NVP]$_o$/[S-(PDLLA$_{15}$-X)$_4$]$_o$ x fraction conversion of NVP(NMR) × mol. wt. of NVP);
[e] Determined from $^1$H NMR by compairing the peak area of the methylene protons of PDLLA block at ~5.2 ppm with that of the methylene proton of PNVP block at ~3.0 - 3.4 ppm;
[f] Determined by GPC (DMF, 0.5 mL/min, 40 $^o$C) calibrated against PMMA standard; [g] $X_{PNVP}$ = mol-fraction of

The observed mole fractions of PNVP blocks in these block copolymers, calculated on the basis of $^1$H NMR and GPC molecular weights, are within the range of

0.35 - 0.62. Observed higher values of PNVP from $^1$H NMR indicates the presence of PNVP homopolymer as impurities. Typical $^1$H NMR spectrum [**Figure 3.3(A)**] of the block copolymer, prepared in **run 1** (**Table 3.2**), in $CDCl_3$, shows, along with the characteristic peaks of the PDLLA block, the presence of the characteristic peaks of the PNVP backbone methine proton '*k*' at ~ 3.5-4.0 ppm, the methylene protons '*l*', '*q*', and '*p*' of the pyrrolidone ring at ~ 3.0 - 3.5, 2.2 - 2.5, and 1.8 - 2.2 ppm, respectively, apart from methylene protons '*j*' of the PNVP block overlapped between at ~ 1.2 and 1.8 ppm with methyl protons '*c*' of PDLLA block. All-star block copolymers were completely soluble in water. All these results indicate the successful occurrence of hetero chain-extension.

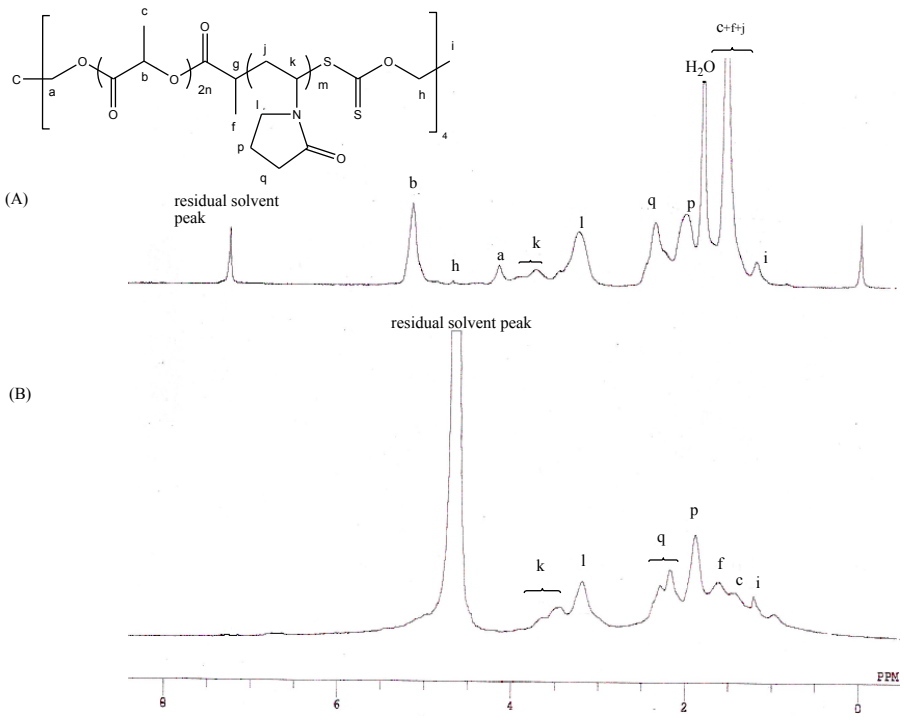


**Figure 3.3** $^1$H NMR spectra of four-arm star block copolymer S-(PDLLA$_{15}$-*b*-PNVP$_{10}$)$_4$ in (**A**) *d*-chloroform and (**B**) $D_2O$ at room temperature.

### 3.3.2 Self-assembly of Amphiphilic S-(PDLLA-*b*-PNVP)$_4$ Block Copolymers in Aqueous Solution

It is well known that amphiphilic block copolymers can form nano-structured micellar aggregates *via* self-assembly. Typical $^1$H NMR spectrum of four-arm star block copolymer S-(PDLLA$_{15}$-*b*-PNVP$_{10}$)$_4$ in $D_2O$ is shown in **Figure 3.3(B)**. Here, the peaks attributed to PDLLA are suppressed in comparison with the $^1$H NMR spectrum obtained in *d*-chloroform [**Figure 3.3(A)**]. This observation indicates the possible formation of micellar aggregates in aqueous solution with PDLLA blocks as the core and PNVP blocks as the shell.

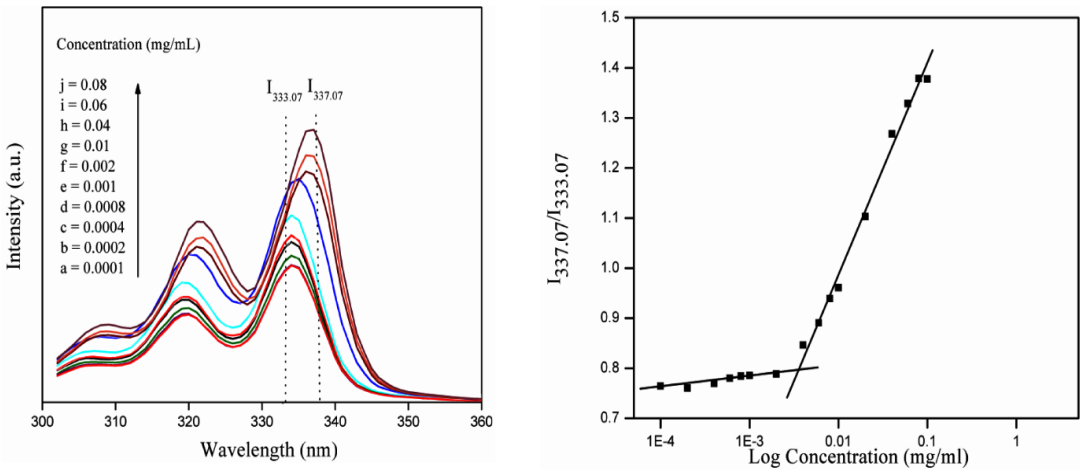


(A) (B)

**Figure 3.4 (A)** Fluorescence excitation spectra (monitored at $\lambda_{em}$ = 394 nm) of pyrene ($6 \times 10^{-7}$ M) in the presence of increasing concentration (C) (mg/mL) of block copolymer S-(PDLLA$_{15}$-*b*-PNVP$_{10}$) (**run 1**, **Table 3.2**) solution in water and **(B)** the corresponding semilogarithmic plot of the fluorescence excitation intensity ratio ($I_{337.07}/I_{333.07}$) of pyrene *vs.* the concentration of polymer.

In order to study the critical micellar concentration (*cmc*) of such four-armed star block copolymers in water, fluorescence spectroscopy is used with pyrene as the probe. Typical fluorescence excitation spectra (300 - 360 nm) of pyrene ($6 \times 10^{-7}$ M) at different S-(PDLLA$_{15}$-*b*-PNVP$_{10}$)$_4$ (**run 1**, **Table 3.2**) concentrations recorded at an emission wavelength of 394 nm are shown in **Figure 3.4 (A)**. **Figure 3.4 (B)** shows the corresponding plot of the $I_{337.07}/I_{333.03}$ intensity ratio (from fluorescence measurements) *vs.* the log of the S-(PDLLA$_{15}$-*b*-PNVP$_{10}$)$_4$ block copolymer's concentration (mg/mL) in water. The observed *cmc*s of the block copolymers S-(PDLLA$_{15}$-*b*-PNVP$_{10}$)$_4$, S-(PDLLA$_{15}$-*b*-PNVP$_{14}$)$_4$ and S-(PDLLA$_{15}$-*b*-PNVP$_{15}$)$_4$ are ~ 3.64 $\times 10^{-3}$, $5.14 \times 10^{-3}$, and $5.81 \times 10^{-3}$ mg/mL, respectively (**Table 3.2**). These values indicate that the *cmc* value of such amphiphilic block copolymers increases with the increase in the chain length of PNVP block. Similar type of results was also reported in the literature. [Mishra *et al*. (2011)] TEM study [**Figure 3.5(a)]** reveals the formation of spherical micellar nanoparticle of average size of 32 nm from the S-(PDLLA$_{15}$-*b*-PNVP$_{10}$) (**run 1**, **Table 3.2**). DLS study reveals that the average hydrodynamic diameter and the PDI of the same star block copolymer (**run 1**, **Table 3.2**) in water are 143.2 nm and 0.432, respectively [**Figure 3.6**].

### 3.3.3 MTX Loading and *In Vitro* Release Study

Methotrexate (MTX) is a poorly water-soluble anticancer drug. It can be encapsulated into the hydrophobic core of the polymeric micelle. The MTX-loaded star (PDLLA$_{15}$-*b*-PNVP$_{10}$)$_4$ polymeric micelles were prepared by using dialysis method. The amount of MTX encapsulated into polymeric micelle was calculated from absorbance of MTX at 308 nm. TEM study clearly shows the larger micellar size for drug-loaded micelle (110

nm dia) with respect to its unloaded micelle (32 nm dia) as expected [**Figure 3.5(b)**]. DLS study shows the larger (263.6 nm with PDI = 0.677) hydrodynamic diameter of the MTX drug-loaded micelle of star S-(PDLLA$_{15}$-*b*-PNVP$_{10}$)$_4$ with respect to that of the parent micelle (143.2 nm with PDI = 0.432*)* [**Figure 3.6**]**.** These results indicate that micelles were successfully loaded with MTX. Indeed, spectroscopic study reveals that MTX-loaded star (PDLLA$_{15}$-*b*-PNVP$_{10}$)$_4$ micelles have the drug loading content of 6.0 % and the drug loading efficiency of 31%.

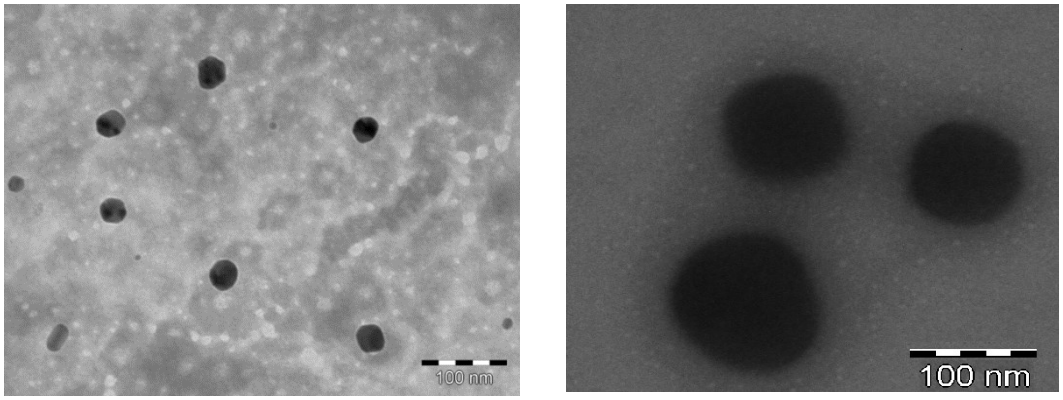


(a) (b)

**Figure 3.5** The TEM images of (**a**) without and (**b**) with MTX drug loaded micelles of S-(PDLLA$_{15}$-*b*-PNVP$_{10}$).

*In vitro* release studies were carried out at 37 $^{o}$C in PBS solutions of pH = 6.4 and 7.4 and release profiles are shown in **Figure 3.7**. These drug-loaded micelles show sustained drug release behavior up to 40.5 and 23% at pH = 6.4 and 7.4, respectively, during initial 24 h. *In vitro* drug release behavior of polymeric micelles is also dependent on the chemical composition of polymeric micelles. In our study, the observed slow drug release in each case may be due to strong interaction between

hydrophobic MTX drug and hydrophobic PDLLA chain length. [Wei *et al*. (2007), Zhang *et al*. (2005)]

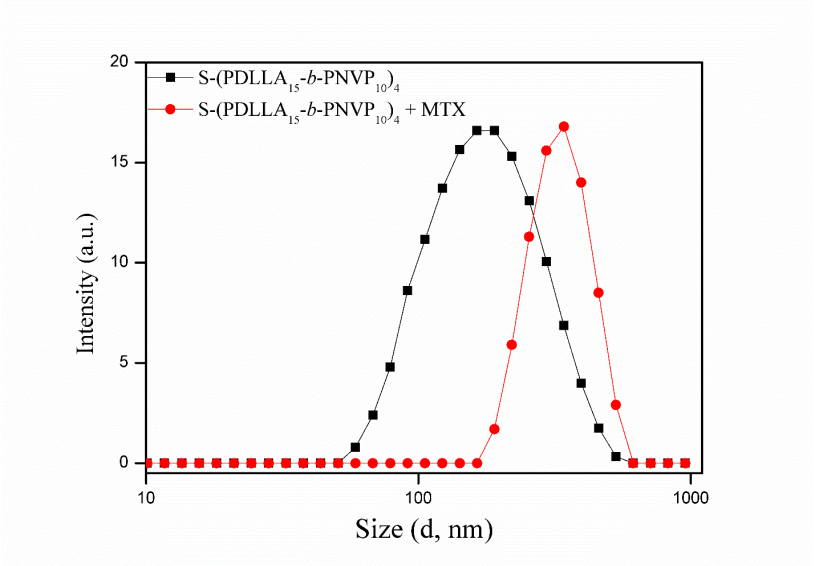


**Figure 3.6** Plot of scattering intensity vs. the effective hydrodynamic diameter of without and with MTX drug loaded micelles of S-(PDLLA$_{15}$-*b*-PNVP$_{10}$) block copolymer at 0.5 mg/mL concentration in water at 90° scattering angle and room temperature.

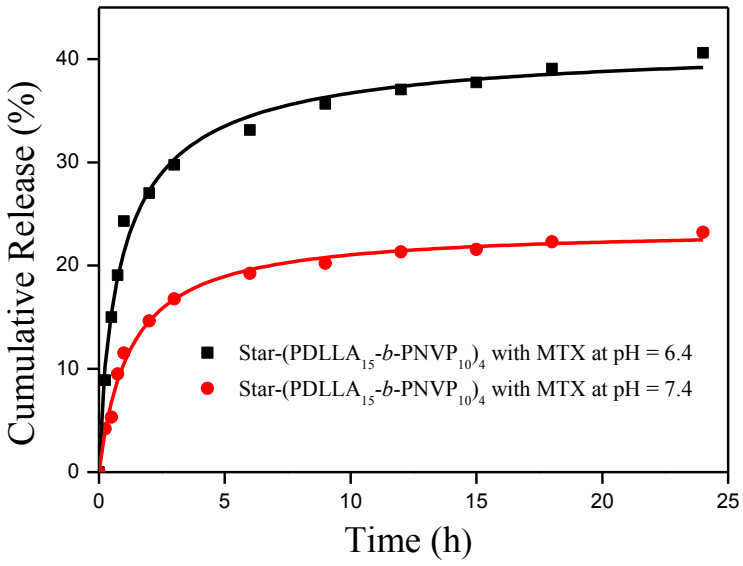


**Figure 3.7** Percentage of cumulative release of MTX from drug-loaded Star-(PDLLA$_{15}$-*b*-PNVP$_{10}$)$_4$ micelles in PBS solution of pH = 6.4 and 7.4 at 37 ºC temperature.

### 3.3.4 Effect of MTX-loaded Star-(PDLLA$_{15}$-b-PNVP$_{10}$)$_4$ on Tumor Cell Viability and Cytotoxicity.

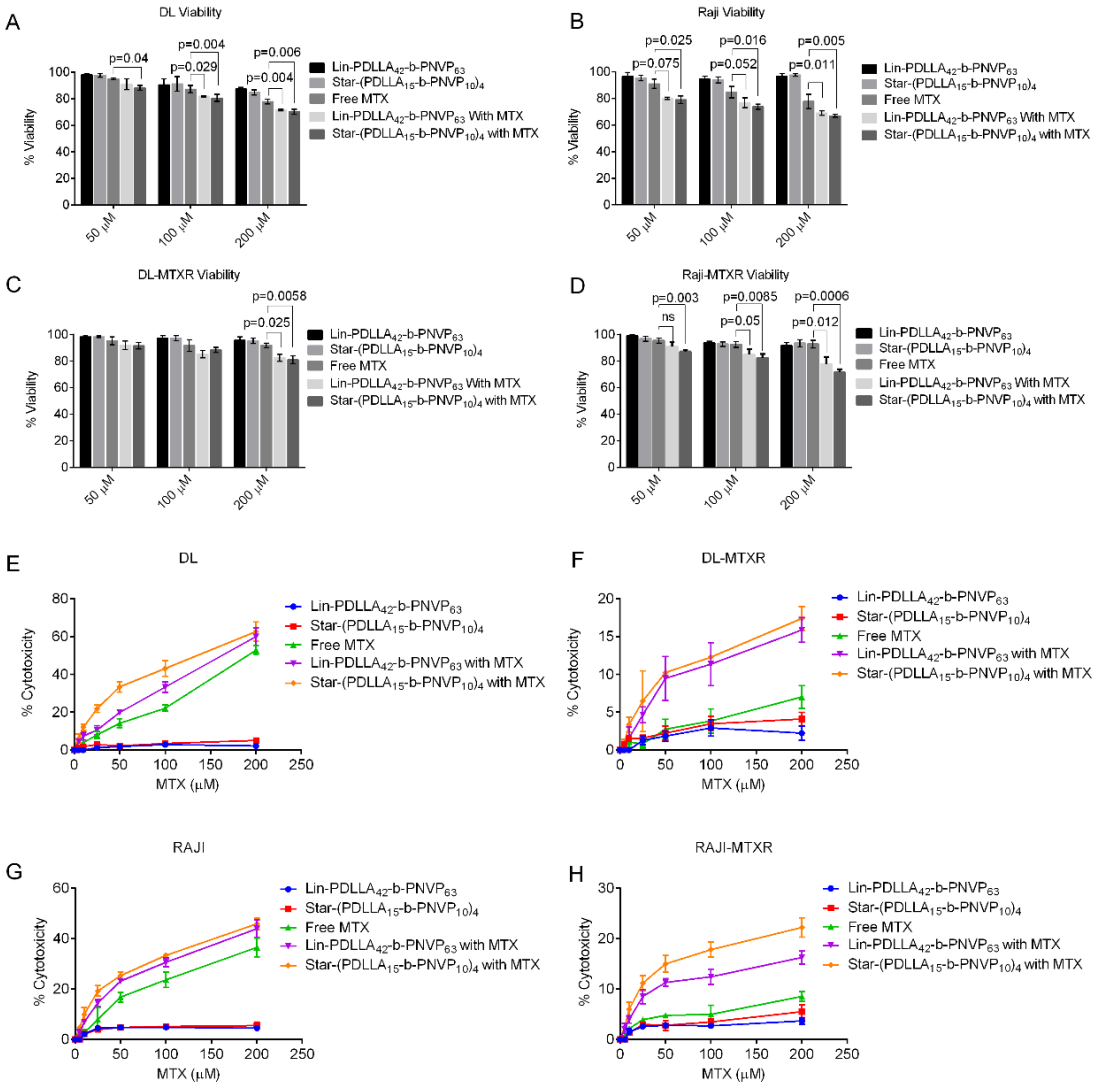


**Figure 3.8** Enhanced killing of tumor cells by star-(PDLLA$_{15}$-*b*-PNVP$_{10}$)$_4$. (**A**, **B**) Viability of parental DL and Raji and (**C**, **D**) MTX resistant DL and Raji cells was studied following XTT viability assay. Cytotoxicity of MTX-loaded star and linear polymers micelles against parental or, MTX resistant DL (**E** and **F**) or, Raji cells (**G** and **H**) was determined by 18 h LDH release assay. Data presented as mean ± SD of triplicate determination, n = 4, where n represents the number of times experiment was performed.

We have performed cell viability and cellular cytotoxicity study for the MTX-loaded Star-(PDLLA$_{15}$-*b*-PNVP$_{10}$)$_4$ amphiphilic block copolymer micelles against parental and MTX-resistant human (Raji) and mouse lymphoma cells (DL) [**Figure 3.8**]. For comparison, the corresponding results of MTX-loaded linear-PDLLA$_{42}$-*b*-PNVP$_{63}$ are also included in the same figure. Compared to free MTX, MTX-loaded star-(PDLLA$_{15}$-*b*-PNVP$_{10}$)$_4$ micelles significantly inhibits the cell viability in a concentration dependent manner. Parental DL (A) and Raji (B) cells responded better with significantly higher loss of cell viability in the presence of MTX-loaded star-(PDLLA$_{15}$-*b*-PNVP$_{10}$)$_4$ micelles compared to free MTX **[Figure 3.8 (A)** and **(B)]**. On the other hand, the MTX resistant DL or, Raji cells are tolerant to free MTX but remain sensitive to MTX-loaded star copolymer micelles [**Figure 3.8 (C)** and **(D)**]. Carrier itself has no effect on the cell viability in any of the cell line tested. This cell viability result was also supported by the susceptibility of human and murine lymphoma cells against MTX-loaded star-(PDLLA$_{15}$-*b*-PNVP$_{10}$)$_4$ micelles with respect to cellular cytotoxicity [**Figure 3.8 (E-H)**]. For comparison, the corresponding results of MTX-loaded linear-PDLLA$_{42}$-*b*-PNVP$_{63}$ are also included in the same figure. MTX-loaded star-(PDLLA$_{15}$-*b*-PNVP$_{10}$)$_4$ amphiphilic block copolymer is highly cytotoxic compared to free MTX at each molar concentrations tested [**Figure 3.8 (E)** and **(G)**]. The carrier it-self does not show cytotoxicity against any of the cell lines tested. Resistant variants of DL and Raji are tolerant to free MTX but remain susceptible to MTX-loaded star-(PDLLA$_{15}$-*b*-PNVP$_{10}$)$_4$ amphiphilic block copolymers at all the concentrations tested **[Figure 3.8 (E)** and **(G)]**. It is clear from the figure that the star-(PDLLA$_{15}$-*b*-PNVP$_{10}$)$_4$ system is more effective than its linear counterpart. This is more evident in MTX resistant Raji cells which are more susceptible to star system compared to its linear

counterpart. Moreover, effectivity increases with increase of their loading (concentration).

### 3.3.5 Cellular Growth Inhibition by MTX-loaded Star-(PDLLA$_{15}$-*b*-PNVP$_{10}$)$_4$

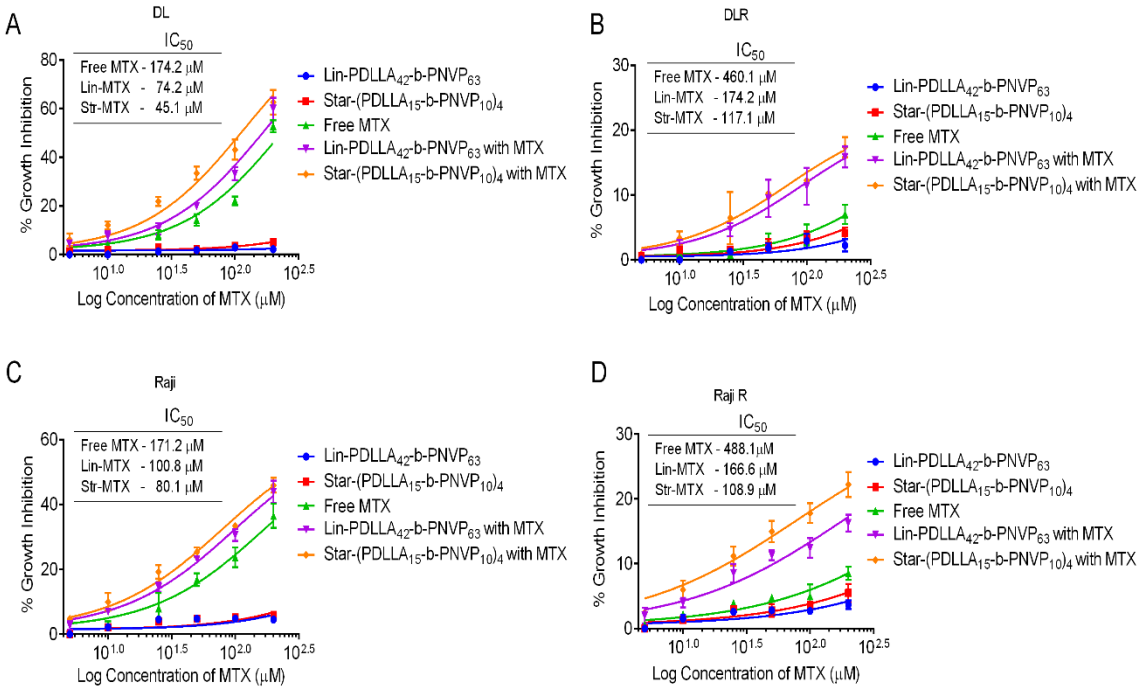


**Figure 3.9** MTX-loaded Star-(PDLLA$_{15}$-*b*-PNVP$_{10}$)$_4$ micelles retard the growth of MTX resistant B cell lymphoma. Graphs show MTX concentration response on cell proliferation and growth after treatment with free MTX, MTX-loaded Star-(PDLLA$_{15}$-*b*-PNVP$_{10}$)$_4$ or, linear PDLLA$_{42}$-*b*-PNVP$_{63}$ micelles in parental and MTX resistant DL (**A** and **B**) or, Burkitt lymphoma cell line Raji (**C** and **D**). Data presented as mean ± SD, n = 5. Differences in IC$_{50}$ values between parental and MTX resistant cell lines are mentioned.

The MTX-loaded star-(PDLLA$_{15}$-*b*-PNVP$_{10}$)$_4$ micelles showed significant growth inhibition against resistant variants of the murine and human lymphoma cells [**Figure 3.9(A)** to **(D)**]. For comparison, the corresponding results of MTX-loaded linear

PDLLA$_{42}$-*b*-PNVP$_{63}$ micellar system are also included in the same figure. Growth inhibition with MTX-loaded star micelles was significantly higher compared to its MTX-loaded linear micelles. $IC_{50}$ for MTX-resistant DL towards free MTX, MTX-loaded linear and star micellar systems increases to 460, 174 and 118 $\mu$M from 174, 74 and 45 $\mu$M, respectively, from their MTX sensitive counterpart [**Figure 3.9(A)** and **(B)**]. Similar results were also observed in MTX resistant Raji cells [**Figure 3.9(C)** and **(D)**]. As observed above, the MTX-loaded star micellar system is more effective compared to the MTX-loaded linear micellar system.

### 3.3.6 Induction of Tumor Cell Apoptosis by MTX-loaded Star-(PDLLA$_{15}$-*b*-PNVP$_{10}$)$_4$ Micelles

Broad spectrum growth inhibition by MTX-loaded star-(PDLLA$_{15}$-*b*-PNVP$_{10}$)$_4$ micelles raises the question whether it also causes apoptosis of tumor cells and if so whether it induces cell death in MTX-resistant tumor cells, which become refractory to any concentrations of MTX. Apoptosis was determined by monitoring changes in cell size and externalization of phosphatidylserine qualitatively in parental and MTX resistant DL to document the events of apoptosis. There was an abundance of Annexin V positive cells in parental DL treated with MTX-loaded star-(PDLLA$_{15}$-*b*-PNVP$_{10}$)$_4$ micelles and comparatively less in MTX-loaded linear PDLLA$_{42}$-*b*-PNVP$_{63}$ micelles (**chapter 2**) which are significantly higher compared to free MTX treatment. Resistant variants of the DL exhibits tolerance to free MTX but become susceptible to MTX-loaded star-(PDLLA$_{15}$-*b*-PNVP$_{10}$)$_4$ micelles [**Figure 3.10 (A)** and **(B)**].

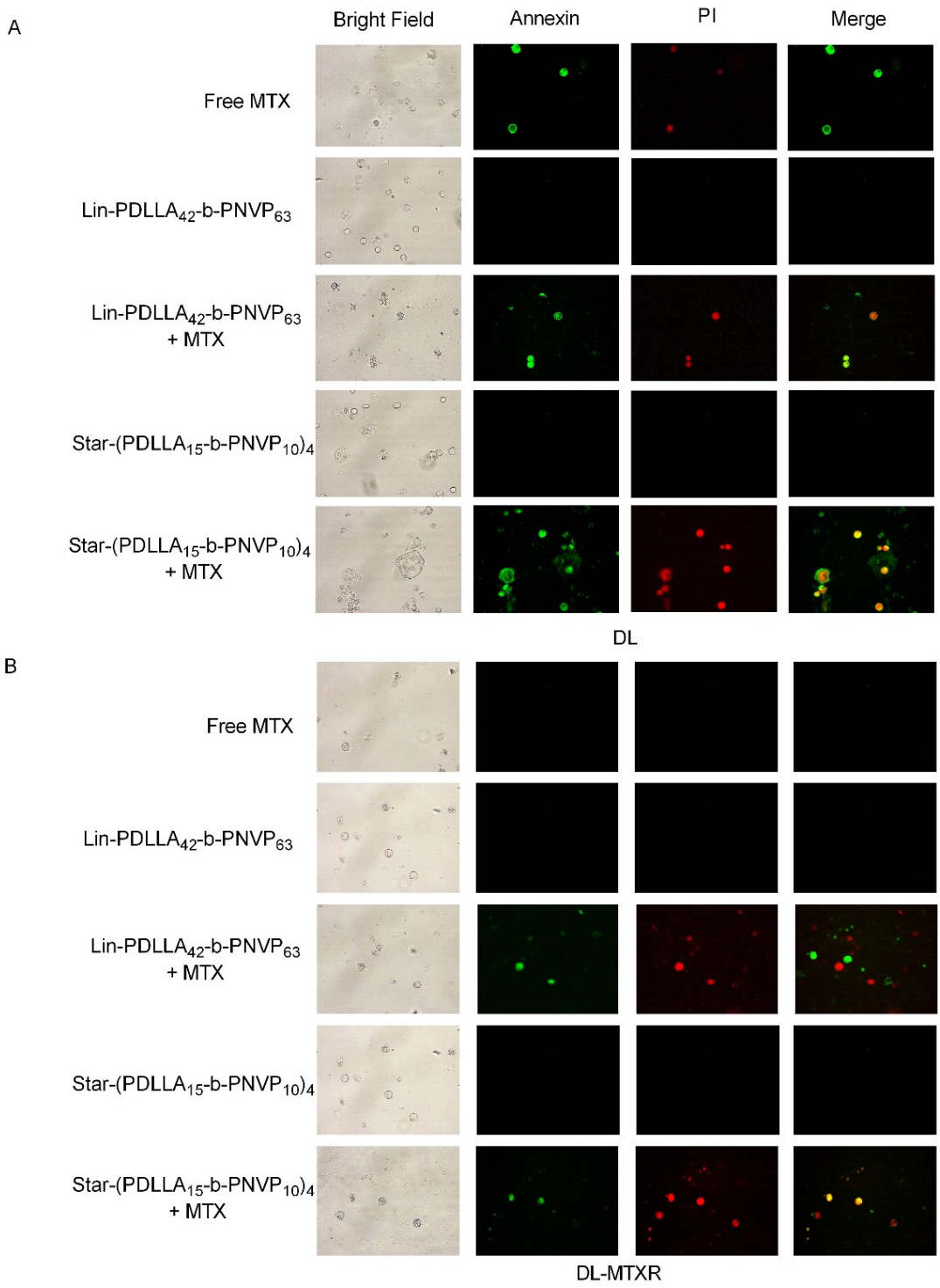


**Figure 3.10** Microscopic analysis of induction of apoptosis in DL. Parental DL (A) and MTX-R/DL (B) Cells were treated with free MTX, free linear PDLLA$_{42}$-*b*-PNVP$_{63}$ and star-(PDLLA$_{15}$-*b*-PNVP$_{10}$)$_4$ block polymers and MTX-loaded linear PDLLA$_{42}$-*b*-PNVP$_{63}$ and star-(PDLLA$_{15}$-*b*-PNVP$_{10}$)$_4$ micelles with equivalent MTX at a concentration of 5.0 $\mu$M. n=4.

### 3.3.7 RBC Integrity and Size Distribution

Like MTX-loaded linear PDLLA$_{42}$-*b*-PNVP$_{63}$ micellar system, MTX-loaded star-(PDLLA$_{15}$-*b*-PNVP$_{10}$)$_4$ micelles did not affect RBC with respect to hemolysis.

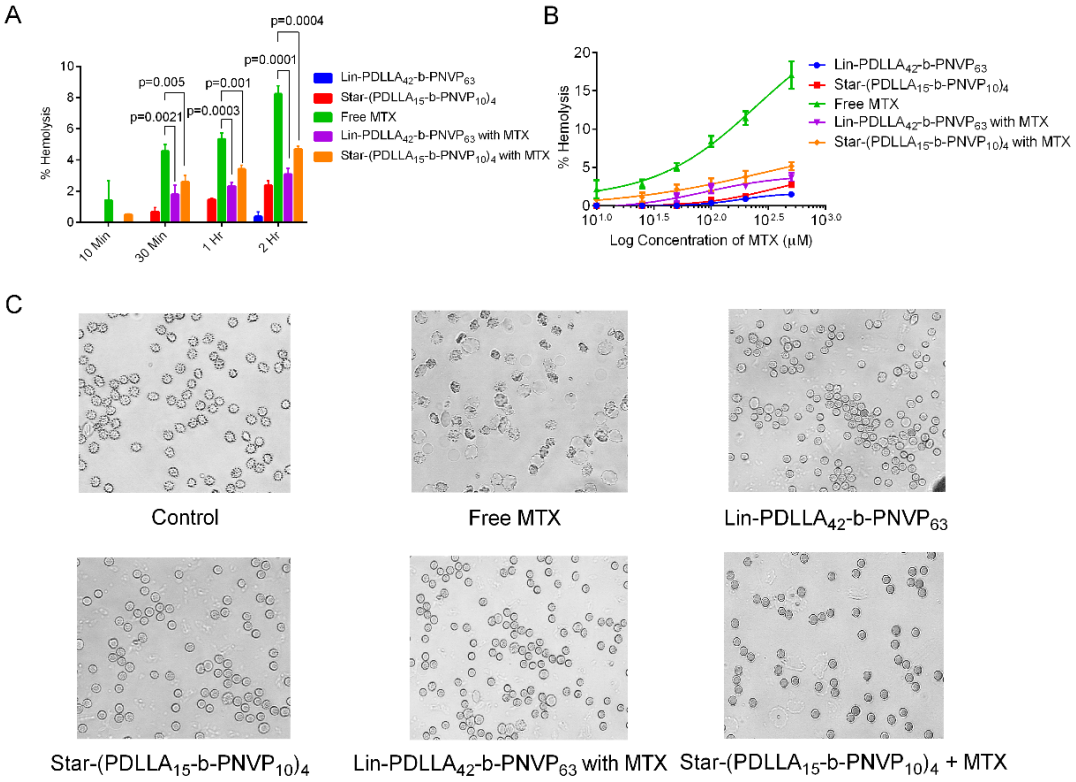


**Figure 3.11** Hemocompatibility assay**.** Hemolysis induced by indicated treatment in whole human blood at a fixed concentration (**A**) or, with increasing concentrations (**B**), and is expressed as percent whole blood hemoglobin content. Mean ± SD, n = 3. Photomicrographs demonstrate the absence of detrimental effect of MTX loaded star-(PDLLA$_{15}$-*b*-PNVP$_{10}$)$_4$ or, linear PDLLA$_{42}$-*b*-PNVP$_{63}$ on RBC morphology compared to MTX treatment alone (**C**).

As a confirmation to RBC counting, hemolysis rate was determined in the presence of the formulations for 4 h which did not exceed the negative control value by more than 2% and, thus the MTX-loaded star-(PDLLA$_{15}$-*b*-PNVP$_{10}$)$_4$ micelles may be

considered as non-hemolytic [**Figure 3.11**]. Hemolysis, studied at increasing time point and concentrations suggests that MTX- loaded star-(PDLLA$_{15}$-*b*-PNVP$_{10}$)$_4$ micelles do not cause damages compared to free MTX which is significantly hemolytic [**Figure 3.11(A)** and **(B)**]. Microscopic observations also demonstrate no change in morphology in RBC following contact with the MTX-loaded star-(PDLLA$_{15}$-*b*-PNVP$_{10}$)$_4$ amphiphilic block copolymers [**Figure 3.11(C)**]. Free MTX on the other hand is significantly hemolytic at all the concentrations tested. Thus, we may conclude that the MTX-loaded linear PDLLA$_{42}$-*b*-PNVP$_{63}$ or, star-(PDLLA$_{15}$-*b*-PNVP$_{10}$)$_4$ amphiphilic block copolymers are tolerant to the RBC, the major cellular component of blood.

### 3.3.8 MTX-loaded Star-(PDLLA$_{15}$-*b*-PNVP$_{10}$)$_4$ Tolerant to Normal Cells

Unlike tumor cells, normal human lymphocytes show tolerance to MTX-loaded star-(PDLLA$_{15}$-*b*-PNVP$_{10}$)$_4$ micelles like MTX-loaded linear PDLLA$_{42}$-*b*-PNVP$_{63}$ micelles [**Figure 3.12**]. Viability of lymphocyte and cellular fractions like dendritic cells (DC) remain unaltered in the presence of MTX loaded amphiphilic block copolymers **[Figure 3.12(A)** and **(B)]**. In contrast, free MTX causes reduction in cell viability of lymphocytes, and DC significantly at comparable molar concentrations of MTX tested (% viability of lymphocytes 60.87 *vs.* 93.26, $p < 0.0001$ at concentration 1 mM) [**Figure 3.12(A)** and **(B)**]. We also checked the direct cytotoxicity of MTX-loaded star-(PDLLA$_{15}$-*b*-PNVP$_{10}$)$_4$ micelles on normal cells and compared with free MTX treatment and MTX-loaded linear PDLLA$_{42}$-*b*-PNVP$_{63}$ micelles. Significantly higher cytotoxicity was observed in lymphocytes or, DC upon treatment with free MTX compared to MTX loaded any of the copolymers at molar concentrations tested [**Figure 3.12(C)** and **(D)**].

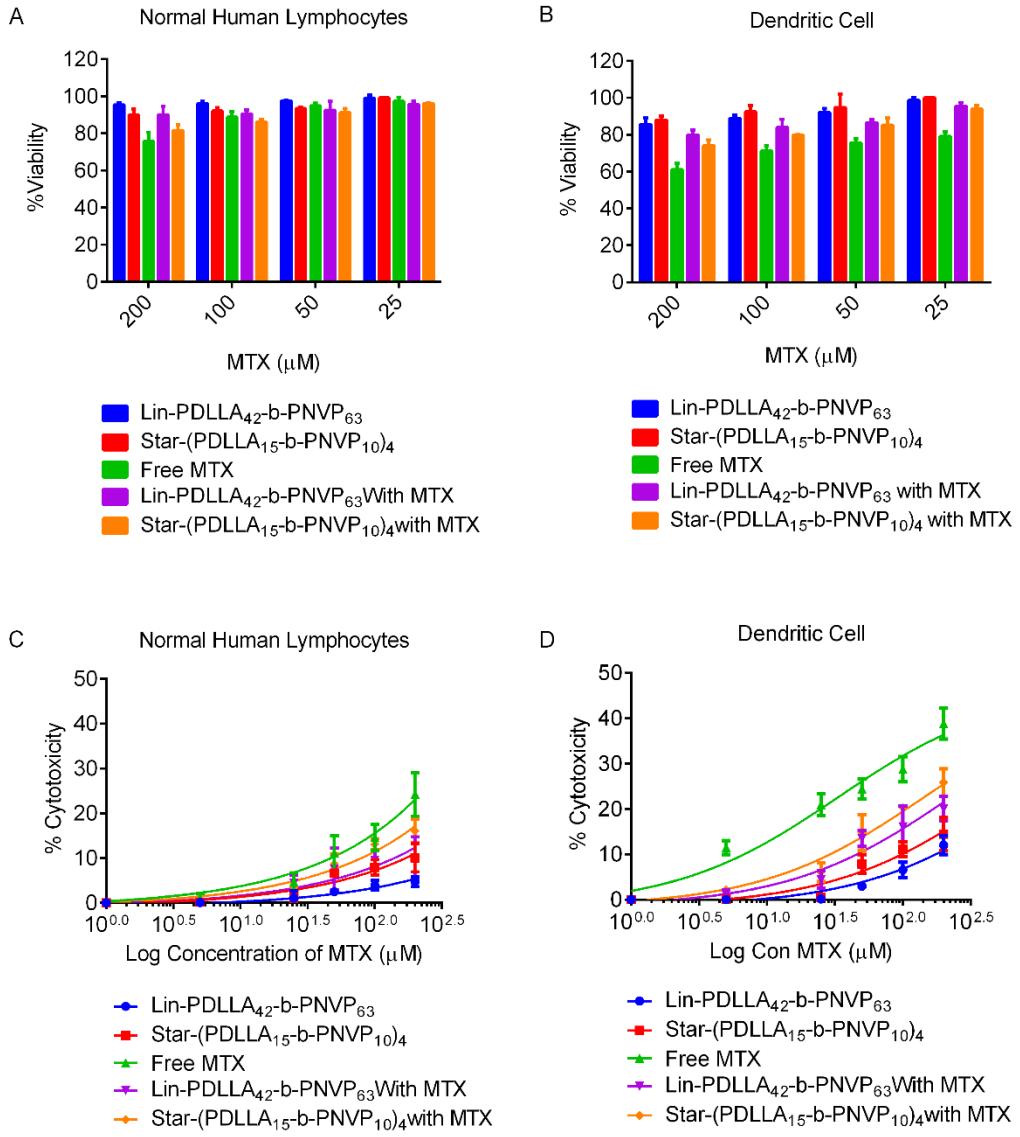


**Figure 3.12** MTX-loaded star-(PDLLA$_{15}$-*b*-PNVP$_{10}$)$_4$ micelles or linear PDLLA$_{42}$-*b*-PNVP$_{63}$ are tolerant to lymphocytes**.** Normal human lymphocytes (**A**) and DC (**B**) were given indicated treatment in complete medium. The cell viability was measured by XTT assay (Cell Signaling, USA). Data shown as Mean ± SD, n = 3. Effects on leukocytes cytotoxicity was determined by 18 h LDH release assay (**C, D**). Data presented as Mean ± SD, n = 4.

These results suggest that normal immune cells are safe in presence of MTX-loaded linear PDLLA$_{42}$-*b*-PNVP$_{63}$ or, star-(PDLLA$_{15}$-*b*-PNVP$_{10}$)$_4$ amphiphilic block copolymer micelles while free MTX significantly harm their potential. Tolerance exhibited by DC to MTX-loaded copolymers compared to free MTX is significant with reference to preservation of intact immune response mediated by DC, may be useful for effective therapeutic response *in vivo* [**Figure 3.12(D)**].

### 3.3.9 Comparative *In Vivo* Antitumor Activity of MTX-loaded linear PDLLA$_{42}$-*b*-PNVP$_{63}$ and star-(PDLLA$_{15}$-*b*-PNVP$_{10}$)$_4$ Micelles

Therapeutic efficacy of MTX-loaded linear PDLLA$_{42}$-*b*-PNVP$_{63}$ or, star-(PDLLA$_{15}$-*b*-PNVP$_{10}$)$_4$ micelles was studied in DL tumor model. Randomly sorted mice (female, 4-6 weeks old) were transplanted with tumor intraperitoneally and were sorted in to 5 groups each with 12 mice. Therapy was started after 96 h post tumor transplant (day 0) [**Figure 3.13(A)**]. Mice of each group were treated with 6 injections of (i) phosphate buffer saline (PBS), (ii) free MTX (3 mg/kg of body weight), (iii) polymer control (vehicle), and (iv) MTX-loaded linear PDLLA$_{42}$-*b*-PNVP$_{63}$ or, star-(PDLLA$_{15}$-*b*-PNVP$_{10}$)$_4$ micelles (equivalent to 3 mg/kg of MTX dose) for every 72 h. The mice injected with PBS or, vehicle control formed large intraperitoneal ascites by day 12 post tumor transplant, which continued with increasing size as the day progresses. Mice treated with free MTX also develops tumor and forms similar ascites at day 20. In contrast, mice treated with MTX-loaded linear PDLLA$_{42}$-*b*-PNVP$_{63}$ or, star-(PDLLA$_{15}$-*b*-PNVP$_{10}$)$_4$ micelles develop tumor at a significantly slower rate and forms similar ascites at day 25. All the mice in PBS and vehicle control groups died between day 20 and 22 from tumor progression. Mice in free MTX group did not survive beyond the

day 25. Tumor bearing mice treated with MTX-loaded linear PDLLA$_{42}$-*b*-PNVP$_{63}$ micelles also did not survive beyond the day 32.

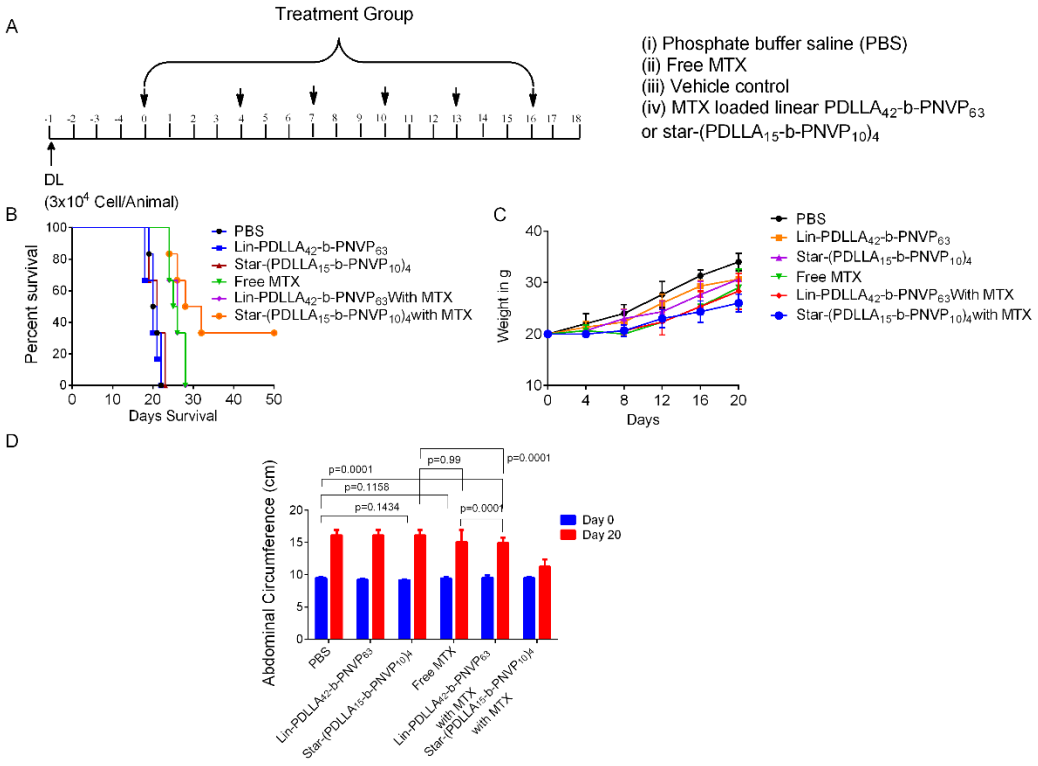


**Figure 3.13 *In vivo* study.** Lymphoma bearing animals were injected with six doses of free MTX, polymer alone, MTX-loaded star-(PDLLA$_{15}$-*b*-PNVP$_{10}$)$_4$ or, linear PDLLA$_{42}$-*b*-PNVP$_{63}$ micelles at a dose of 3 mg kg$^{-1}$ MTX of body weight as indicated by the arrows for 3 weeks (**A**). The animals in the study responded better to the therapy with MTX-loaded star-(PDLLA$_{15}$-*b*- PNVP$_{10}$)$_4$. Kaplan-Mayer survival analysis was performed following therapy and was analyzed for the percent survival up to day 50 post tumor transplant by log-rank test using Graph Pad PRISM software (**B**). Body weight (**C**) and, abdominal circumference (**D**) were determined for the indicated treatment.

In contrast, 4 of 12 mice in the MTX-loaded star-(PDLLA$_{15}$-*b*-PNVP$_{10}$)$_4$ micelles group were alive at day 50 when the experiment was terminated. Kaplan-Mayer survival analysis shows prolong survival of MTX-loaded star-(PDLLA$_{15}$-*b*-

$PNVP_{10})_4$ group compared to free MTX treatment or, treatment with MTX-loaded linear $PDLLA_{42}$-*b*-$PNVP_{63}$ groups [**Figure 3.13(B)]**.

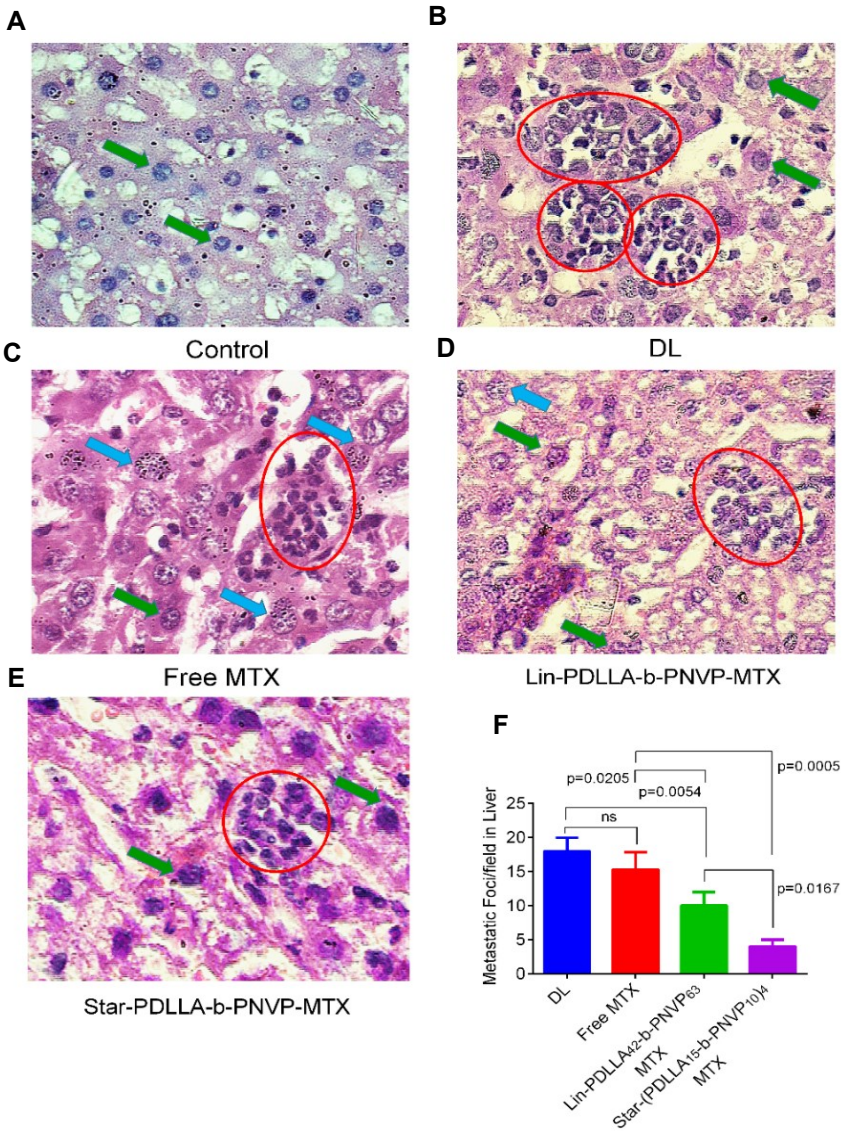


**Figure 3.14** MTX-loaded star-$(PDLLA_{15}$-*b*-$PNVP_{10})_4$ or, linear $PDLLA_{42}$-*b*-$PNVP_{63}$ micelles protect metastasis. Haematoxylin and eosin staining of liver tissues derived from (A) healthy untreated DL tumor bearing mice or, treated groups (**B**, **C**, **D**, **E**) are shown. In liver, metastatic lymphoid cells (red circle) are shown (**F**). Tumor metastatic foci/fields (arrows) were counted in untreated and in mice with indicate treatment. Mean ±SD, n = 4.

This result is in agreement with a distinct reduction in body weight and abdominal circumference in MTX-loaded star-(PDLLA$_{15}$-*b*-PNVP$_{10}$)$_4$ micelles treatment (average 26 g/mice), compared to vehicle control (average 38 g/mice) or, free MTX treated mice (average 35 g/mice) [**Figure 3.13 (C)** and **(D)**].

Validation of therapeutic efficacy of MTX-loaded star-(PDLLA$_{15}$-*b*-PNVP$_{10}$)$_4$ micellar system in DL tumor model resulted in dramatic growth inhibition and prevention of metastasis, indicating the increase in therapeutic index of the formulation. Histopathological analysis of liver clearly indicates the efficacy of the formulation in restricting the metastasis of the organs [**Figure 3.14 (A - E)**]. In liver, infiltrated metastatic lymphoid cell (red circle) are clearly visible in DL mice which are significantly reduced in mice treated with MTX-loaded star-(PDLLA$_{15}$-*b*-PNVP$_{10}$)$_4$ in comparison to MTX-loaded linear system. Counting of metastatic foci and metastatic field in liver sections also clearly suggest a significant reduction in metastasis following therapy with MTX-loaded star-(PDLLA$_{15}$-*b*-PNVP$_{10}$)$_4$ micellar system ($p = 0.0005$ between MTX and treatment in liver) [**Figure 3.14(F)**].

## 3.4 Conclusions

We have successfully synthesized well-defined four-arm star amphiphilic block copolymers consist of PDLLA and PNVP blocks *via* the combination of ROP and xanthate-mediated RAFT polymerization. Synthesized polymers were characterized by $^1$H NMR spectroscopy and GPC. The amphiphilic four-arm star block copolymer forms spherical micelles in water as evidenced by TEM, $^1$H NMR spectroscopy, and DLS studies. The critical micellar concentrations of these block copolymers were determined by fluorescence spectroscopy using pyrene as a probe. Methotrexate (MTX)-loaded

polymeric micelle of star-(PDLLA$_{15}$-*b*-PNVP$_{10}$)$_4$ amphiphilic block copolymers, with drug loading content of 6.0 % and loading efficiency of 31%, were prepared and characterized by UV-Vis, DLS and TEM studies. The size of polymeric micelles increased from 32 nm to 110 nm in diameter after drug loading. Sustained drug release properties have been shown by MTX-loaded Star-(PDLLA$_{15}$-*b*-PNVP$_{10}$)$_4$.Drug loaded polymeric micelles of both star and linear amphiphilic block copolymers show significant growth inhibition, cytotoxicity, and apoptosis of DL and Raji cells. MTX-loaded star micellar system also show antitumor activity against MTX resistant DL and Raji cells while free MTX is ineffective. Moreover, this system does not cause hemolysis of RBC while free MTX causes significant hemolysis. Star-(PDLLA$_{15}$-*b*-PNVP$_{10}$)$_4$ amphiphilic block copolymer performs better than its linear counterpart. Tumor bearing mice treated with MTX-loaded star-(PDLLA$_{15}$-*b*-PNVP$_{10}$)$_4$ amphiphilic block copolymers prolongs the survival of mice with active disease responded against DL which was significantly impaired in untreated tumor bearing mice. Compared to linear copolymer, the star form demonstrates superior performance with reference to antitumor activity.